

Pressure dependence of Na resonance line broadening by Kr and Xe

W. P. West* and Alan Gallagher†

Joint Institute for Laboratory Astrophysics, University of Colorado and National Bureau of Standards, Boulder, Colorado 80309

(Received 3 October 1977)

The fluorescent spectrum of the Na *D* lines, pressure broadened by Xe and Kr, has been measured for noble-gas densities of 2×10^{19} – 3×10^{20} cm⁻³; at the lower density, the lines are isolated while, at the higher, they are severely blended. The spectra are obtained in normalized intensity units allowing the nonbinary behavior of the line wing intensity to be clearly observed. At the lower density the broadening is well characterized by isolated binary interactions; at the higher density multiple-perturber interactions dominate. Nonlinearities in the pressure dependence of shifts, widths, and satellite shape are reported.

I. INTRODUCTION

The theory of collisionally broadened atomic line shapes in low-pressure gases is relatively well developed. The line shape depends on atomic interaction energies that are frequently poorly known, but methods for calculation of a line shape in terms of these interactions are well established.¹⁻⁴ Primarily, the impact approximation is used to calculate the width and shift of the Lorentzian line core and the quasistatic approximation is used for the far wings with certain improvements²⁻⁶ in the neighborhood of "satellites," or intensity maxima in the line wings. The transition between "line core" and "far wing" occurs at $(\omega - \omega_0)\tau_c \cong 1$, where τ_c is the characteristic collision time, ω photon frequency, and ω_0 the unperturbed atomic frequency.

The problem of describing line shapes at high pressures, with overlapping collisions and multi-body interactions, is quite formidable. The impact approximation is not applicable in the line core and even the simple quasistatic theory requires a number of additional assumptions of questionable validity in order to be applicable in the far wings.

The quantum-mechanical improvements to the quasistatic theory in the neighborhood of satellites^{2,5,6} (see Ref. 7 for a recent review) are limited to nonoverlapping interactions (low pressures). One method that is applicable in all parts of the line at all densities is the Anderson-Talman-type semiclassical theory,⁹ which utilizes the Fourier transform of the autocorrelation function. Calculations^{3,9-11} based on this theory have utilized the approximations (i) that multiple-perturber interactions are uncorrelated and can be represented by scalarly additive identical radiator-perturber-pair interactions; (ii) that no nonadiabatic mixing of (effectively) molecular adiabatic states occurs; (iii) that the quantum-mechanical effects associated with turning points and quasibound or bound states

be neglected; and (iv) straight-line collision orbits. Other, related theories^{12,13} do not remove any of these assumptions, while treatments of nonadditive interactions are so far too formal to yield quantitative results.^{14,15} The additivity assumption for different perturbers has been tested in one case.¹⁶ In practice, only Refs. 3, 9-11, based on the Anderson-Talman-type theory, have calculated a high-pressure spectrum from interaction potentials, and they have utilized further approximations due to the severe computational difficulties. All these calculations have assumed a single-excited and ground-state binary interaction potential, which is rarely valid (a $^2S_{1/2}$ - $^2P_{1/2}$ transition, where the $^2P_{1/2}$ - $^2P_{3/2}$ fine-structure is large, is an exception). Further, Ref. 10 utilized an unrealistic square-well potential and Ref. 9 investigated only a single interaction potential. Kielkopf³ carefully investigated the computational difficulties as well as a number of interatomic potentials, although he concentrated primarily on certain satellite shapes. This recent work represents most of our present understanding of high-pressure line shape, yet only a few qualitative conclusions of Ref. 3 are applicable to any specific transitions other than those studied therein. Furthermore, the above assumptions used so far in evaluating the Anderson-Talman theory are of questionable validity; in particular the single-potential approximation is completely inappropriate in the present case.

The inaccuracies resulting from the assumptions utilized in the theories are largely untested since, as noted in Ref. 3, available data are not sufficiently restrictive. In fact, the theories have sufficient free potential parameters to readily fit a single measured line shape,⁹ satellite shape,^{3,10} or the pressure-dependence of the line-core shift and width. Clearly, comprehensive data for systems with known interaction potentials are needed.

It is the purpose of this work to provide accurate quantitative data for the pressure dependence of

the line shape in the region of the D lines and a nearby red satellite. Furthermore, we have chosen a case for which the binary-pair interactions are relatively well known from theory¹⁷⁻¹⁹ and experiment.^{20, 21}

At the lowest pressures studied, the line shape is predominantly due to binary interactions, and at the highest pressures the D lines have essentially disappeared. The line shape is analyzed to obtain the pressure dependence of the D -line shifts and widths, but there are no calculations available to which these results can be compared. The dependence of the satellite shape on pressure is reported, but again no calculation is presently available for comparison. We have studied the region just beyond the satellite to search for a "secondary" satellite due to NaXe_2 , and made quantitative comparisons to theoretical predictions based on the additive-potential model.

For the perturber densities $[\text{Xe}]$ of these experiments, the extreme wing intensities, at frequency shifts in excess of 100 cm^{-1} , are predominantly due to only one- and two-perturber interactions or to NaXe and NaXe_2 spectra. There are no satellites on the extreme red wing and the relatively simple, quasistatic, additive-pair interaction theory for the NaXe_2 spectra can be tested there. We have made detailed comparisons of the extreme-wing data to the predictions of this theory in a separate publication.²²

II. EXPERIMENT AND RESULTS

The fluorescence spectrum of optically excited $\text{Na}(3P)$ in the presence of Xe and Kr was measured. The cell temperature was 450 K and the sodium density $[\text{Na}]$ was below its equilibrium value. Details of the apparatus are given in Ref. 22. The Na vapor was optically thin ($[\text{Na}] < 10^{11} \text{ cm}^{-3}$) and the total emission spectrum without radiation entrapment was measured. In order to obtain fluorescence signals without interference from instrumental and Rayleigh scattering, the cw dye laser ($\sim 1 \text{ W/cm}^2$ in 0.01 nm) used to excite the $\text{Na}(3P)$ was tuned to various wavelengths 0.1–0.5 nm in the wings of the broadened resonance lines. Scattering at the laser wavelength are ignored and all portions of the emission spectrum are obtained by measuring the spectrum for different laser wavelengths. Three-photon scattering²³ was not observed, as expected for our weak laser power density. At the noble-gas densities of the experiment essentially complete spectral redistribution and $^2P_{1/2} \leftrightarrow ^2P_{3/2}$ mixing occurs, and the fluorescence spectrum is independent of the exciting wavelength.

The results are reported as $I_N(k)$, the normal-

ized emission intensities per cm^{-1} interval divided by noble-gas density $[\text{Xe}]$ or $[\text{Kr}]$,

$$I_N(k) = \frac{I(k)}{[\text{Xe}] \int I(k) (k_0/k)^4 dk} \quad (1)$$

where $I(k)$ is the measured fluorescence intensity per cm^{-1} interval, in arbitrary units. At low $[\text{Xe}]$ most of the integral results from the D lines while the line-wing intensity is predominantly due to binary Na-Xe interactions and is a constant in such a plot. In the wing of a Lorentzian line with broadened width $\gamma \propto [\text{Xe}]$, $I_N(k)$ is constant at all $[\text{Xe}]$. Departures from this behavior are observed in the line wings reported below. The $(k_0/k)^4$ factor in the normalization integral is a relatively minor factor that gives a physical meaning to the integral. As shown in Ref. 22, this integral equals $hck_0\Gamma_0[\text{Na}_T^*]$, where k_0 is the D -line centroid frequency, Γ_0 the spontaneous emission rate, and $[\text{Na}_T^*]$ the total concentration of excited $\text{Na}(3p)$ in all bound and free forms.

In Fig. 1 the line-center data are given for a number of Xe densities. The rms fluctuation in individual points is $\sim 2\%$, while the absolute normalization is accurate to $\sim 5\%$. A number of redundant data sets were taken in the 587–593 nm region to search for any regular intensity undulations. Such undulations are known to occur in the neighborhood of some satellite structures for low²⁴ or high²⁵ perturber pressures. One calculation has indicated that such undulations might occur at high perturber pressures even though they do not occur at low pressures.¹⁹ A "satellite" structure appears in Fig. 1 as a $\sim 591 \text{ nm}$ red edge to the relatively constant intensity 590–591 nm region, however, *no intensity undulations were discerned anywhere in the 587–593 nm wavelength for any $[\text{Xe}]$* . The upper limit on the fractional change in any undulations is set by the experiment at $\sim 1\%$. Another, much weaker satellite occurs on the blue wing at $\sim 559 \text{ nm}$ (Fig. 2). The lower intensity of this satellite precluded an equivalent search for undulatory structure in its wavelength region. In Fig. 2 the entire measured spectrum is plotted on a log-log scale to give an overview of the entire line wings. The $\Delta k = -100$ to -2500 cm^{-1} region is the $\text{Na}^*\text{Xe } A\text{-X}$ band²¹; its red edge at $\Delta k \cong -2200 \text{ cm}^{-1}$ is not a satellite, rather it is due to the effect of the repulsive inner wall of the A -state potential on the perturber distribution.²¹ The pressure dependence of the $\Delta k = -300$ to -4500 cm^{-1} region is the subject of Ref. 22 and is not discussed here.

The red-wing region is shown in Fig. 3 for several krypton densities. As with xenon, the pressure dependence of the $\Delta k < -100 \text{ cm}^{-1}$ region is

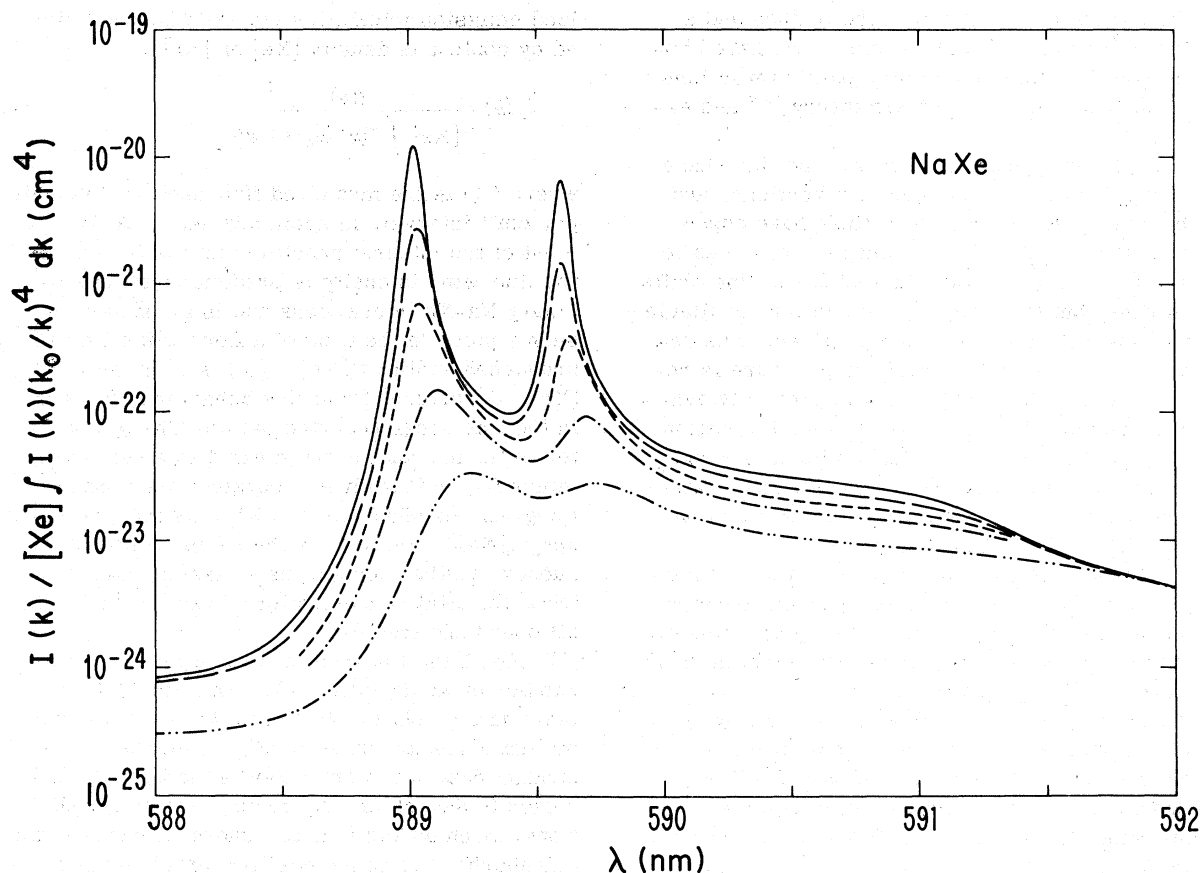


FIG. 1. Normalized fluorescence of optically thin Na at 450 K in the presence of Xe densities of $2.18 \times 10^{19} \text{ cm}^{-3}$ (solid line), $5.45 \times 10^{19} \text{ cm}^{-3}$ (long dashes), $1.06 \times 10^{20} \text{ cm}^{-3}$ (short dashes), $1.83 \times 10^{20} \text{ cm}^{-3}$ (dash-dot), and $3.20 \times 10^{20} \text{ cm}^{-3}$ (dash-double-dot). The spectrometer resolution was 0.05 nm. The lines are drawn through the average of individual data points (not indicated) at 0.02 nm intervals; individual points scatter $\sim 2\%$ rms about the averages.

covered in Ref. 22. A severely blended "satellite" occurs at $\Delta k \cong -30 \text{ cm}^{-1}$. Note that the normalized intensity between λ_0 and the satellite decreases with increasing [Kr], as it did for Xe in Figs. 1 and 2. However, at $-30 \text{ cm}^{-1} < -80 \text{ cm}^{-1}$, past the satellite, the intensity increases with increasing [Kr], whereas for Xe (Fig. 2) the normalized emission coefficient was essentially independent of [Xe] in that region of the spectra. Again, no undulations in the spectra were apparent in the region of the satellite.

The normalized emission coefficient $I_N(k)$ at the lowest density of $2.18 \times 10^{19} \text{ cm}^{-3}$ is given in Fig. 4, where it is compared to previous absorption measurements by McCarten and Farr.²⁶ At the 10^{18} – 10^{19} cm^{-3} perturber densities of Ref. 24, the broadening of the two $\text{Na}(^2P_{1/2,3/2})$ lines is small enough that the lines can be considered independently. Their measured $P_{1/2}$ -line absorption wing shape has been converted to a spontaneous emission wing shape by multiplying by

$(k/k_0)^3 \exp[-hc(k-k_0)/k_B T]$, where k_B is the Boltzmann constant (e.g., see Ref. 21). It has been put in absolute units by connecting it at $|\Delta k| \leq 1 \text{ cm}^{-1}$, where it has a Lorentzian shape, to the $P_{1/2}$ -line Lorentzian line wing. The Lorentzian wing intensity for an isolated line of full width γ is given in $I_N(k)$ units, in terms of $\gamma/[\text{Xe}]$, by

$$\frac{I(k)}{[\text{Xe}] \int I(k) (k_0/k)^4 dk} = \frac{(k/k_0)^4 (2\pi)^{-1} (\gamma/[\text{Xe}])}{(k-k_0-d)^2 + (\gamma/2[\text{Xe}])^2} \quad (2)$$

The $P_{3/2}$ and $P_{1/2}$ states will be populated in the thermal ratio $2 \exp(-17 \text{ cm}^{-1}/k_B T) = 1.89$ due to Xe collisional mixing, and they radiate at the same rate. Thus, as we have normalized our data to the emission integrated across both $P_{1/2}$ and $P_{3/2}$ lines, and at this $[\text{Xe}] \cong 2 \times 10^{19} \text{ cm}^{-3}$ almost all of the emission is in the lines (Fig. 1), the $I_N(k)$ of Eq. (2), for the $P_{1/2}$ line only, must be multiplied

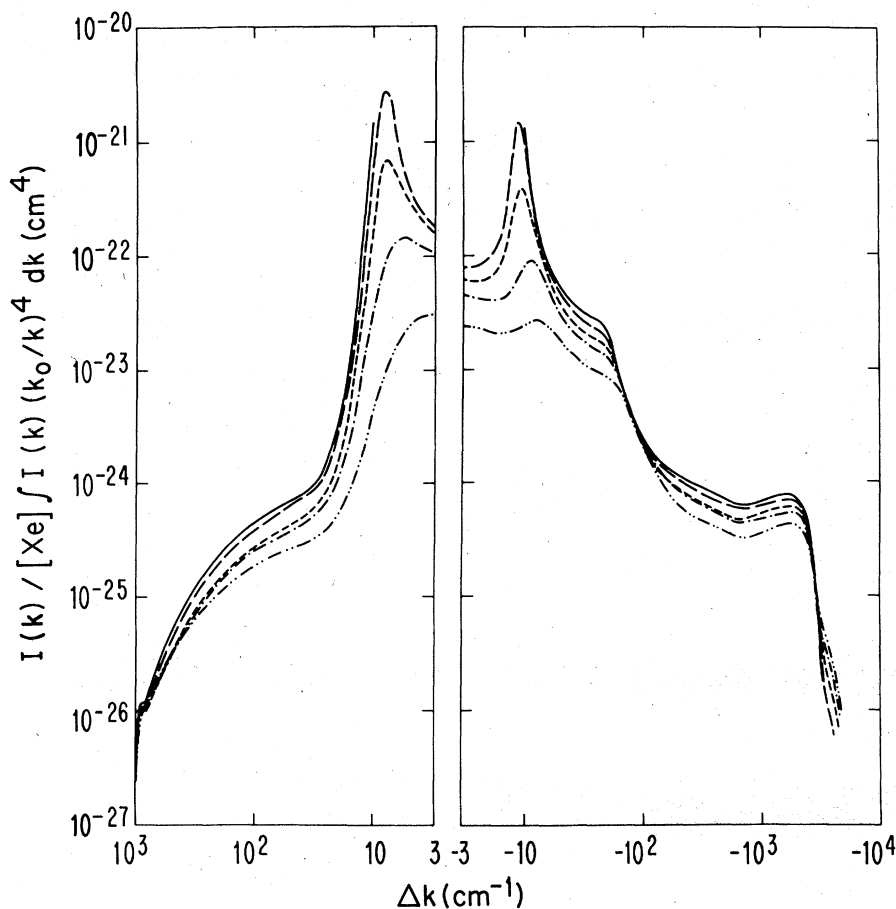


FIG. 2. Same as Fig. 1, except that the spectrometer resolution decreases to ~ 1 nm for $|\Delta k| > 300$ cm^{-1} and data points are at wider intervals at the larger $|\Delta k|$.

by $1/2.89$ for the comparison to our data. As shown in Fig. 4, the resulting $I_N(k)$ calculated using the (full width) $\gamma/[\text{Xe}]$ of the $P_{1/2}$ line measured by McCarten and Farr has about the same shape as the present measurement but is lower by a factor of ~ 1.6 . A 36% larger value of $\gamma/[\text{Xe}]$, and thus of $I_N(k)$, has recently been calculated by Lwin *et al.*¹⁹ As shown in Fig. 4, if the wing shape reported in Ref. 24 is normalized to the Lorentzian wing according to the procedure described above using their calculated $\gamma/[\text{Xe}]$, the agreement with the present results is much better ($\sim 20\%$). Lwin, McCarten, and Lewis¹⁹ have suggested that the $\gamma/[\text{Xe}]$ measured by McCarten and Farr²⁶ may be in error in the case of xenon and the present data support that suggestion. We are not aware of any other measurements of Xe broadening of these Na lines.

The full widths at half maximum (FWHM) of the Xe broadened $P_{1/2}$ (589.6 nm) and $P_{3/2}$ (589.0 nm) lines were measured with an instrument resolution $\Delta = 0.03$ nm at the lower $[\text{Xe}]$ and 0.05 nm for the higher $[\text{Xe}]$. The observed widths (W) of ≥ 0.6 nm were corrected by (5–30)% for the instrumental

contribution using the approximation $\gamma = (W^2 - \Delta^2)^{0.5}$. The shifts (d) of the peak positions of these two lines were measured relative to a low-pressure sodium discharge lamp. Since the measurement of the shifts involves only the determination of the peak positions, the uncertainties are deemed to be significantly less than the instrumental resolution and are ± 0.003 nm at the lower $[\text{Xe}]$ and ± 0.01 nm at the higher $[\text{Xe}]$. At low $[\text{Xe}]$, γ and d are proportional to $[\text{Xe}]$, so we have plotted $\gamma/[\text{Xe}]$ and $d/[\text{Xe}]$ vs $[\text{Xe}]$ in Fig. 5 to indicate departures from low-pressure behavior. The low-pressure limiting values of $d/[\text{Xe}]$ shown in Fig. 5 have been measured by McCarten and Farr,²⁶ while both the calculated¹⁹ and measured²⁶ limiting values of $\gamma/[\text{Xe}]$ are shown. The uncertainty in the widths obtained in the present low-resolution measurements includes uncertainty in the above correction for instrumental broadening.

III. DISCUSSION

The general pattern of the data in Figs. 1 and 2 is a broadening and red shift of the D lines with

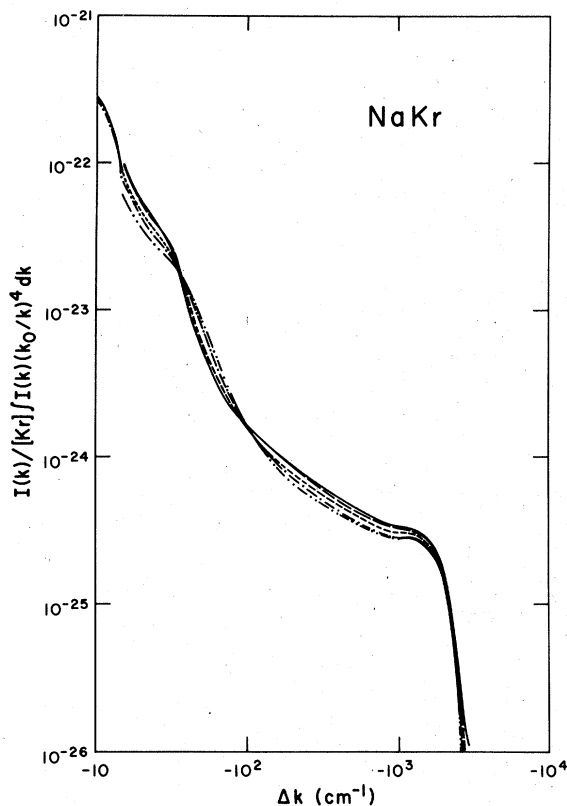


FIG. 3. Normalized fluorescence of optically thin Na at 450 K in the presence of Kr densities of $2.02 \times 10^{19} \text{ cm}^{-3}$ (solid line), $5.21 \times 10^{19} \text{ cm}^{-3}$ (long dashes), $1.04 \times 10^{20} \text{ cm}^{-3}$ (short dashes), $2.10 \times 10^{20} \text{ cm}^{-3}$ (dash-dot), and $3.16 \times 10^{20} \text{ cm}^{-3}$ (dash-double-dot).

increasing $[\text{Xe}]$. The intensity in the line centers decreases relative to that in the wings until they merge and the lines disappear. It is useful to recognize that a single isolated Lorentzian line would have a normalized intensity $I_N(k)$ given by Eq. (2). Thus, if $\gamma/[\text{Xe}]$ were a constant, the width of the line would be proportional to $[\text{Xe}]$, the normalized line peak would decrease as $[\text{Xe}]^{-2}$, and the wings would appear constant (the area decreases as $[\text{Xe}]^{-1}$ by definition). Such a constant wing intensity and $\gamma/[\text{Xe}]$ is consistent with a binary (Na-Xe) interaction only. At low $[\text{Xe}]$ the normalized wing intensities are indeed independent of $[\text{Xe}]$, but at the high $[\text{Xe}]$ of these experiments the normalized line-wing intensities generally decrease with increasing $[\text{Xe}]$. This is caused by the depletion of free Na^* atoms due to molecular formation and the fact that multibody interactions (Na^*Xe_n , $n=2, 3, \dots$) spread the intensity into other portions of the spectrum. In essence, according to the Poisson distribution, the probability of one and only one Xe in a particular volume ΔV about a Na^* is given by $\Delta V[\text{Xe}] \exp(-\Delta V[\text{Xe}])$. Here the

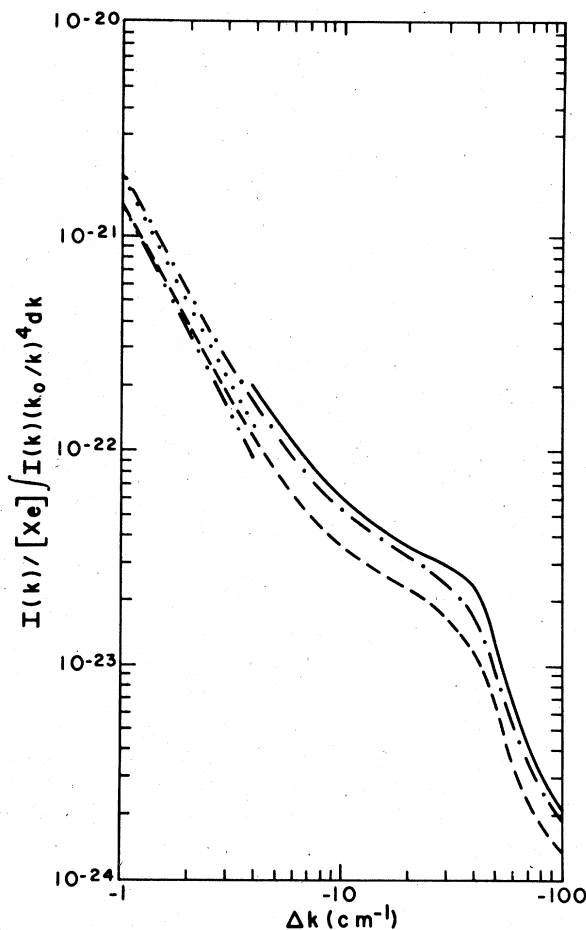


FIG. 4. Normalized fluorescence of Na at 450–460 K in the presence of Xe. Present data at $[\text{Xe}] = 2.2 \times 10^{19} \text{ cm}^{-3}$ (solid line). Data of McCarten and Farr²⁶ normalized to their measured broadening coefficient $\gamma/[\text{Xe}] = 2.79 \times 10^{-20} \text{ cm}^2$ (short dashes) and the calculated¹⁹ broadening coefficient $\gamma/[\text{Xe}] = 3.78 \times 10^{-20} \text{ cm}^2$ (dash-dot). Also shown are the pure Lorentzian shapes (dash-double-dot) and (dotted), for these two values of $\gamma/[\text{Xe}]$. Δk is measured from the center of the (unperturbed) D_1 line.

probability of remaining a free Na^* with no Xe inside ΔV is $\exp(-\Delta V[\text{Xe}])$, and the remaining probability is accounted for by multiple-Xe interactions. A more complete discussion of these multibody contributions to the wing spectrum is contained in Ref. 22.

A. Shift and width

The shifts and FWHM of the D lines were plotted as $d/[\text{Xe}]$ and $\gamma/[\text{Xe}]$ vs $[\text{Xe}]$ in Fig. 5. The low-pressure limit of the broadening rate $\gamma/[\text{Xe}]$ is uncertain by about $\pm 30\%$ due to the disagreement between the present data and Ref. 26, but within this uncertainty $\gamma/[\text{Xe}]$ does not appear to vary

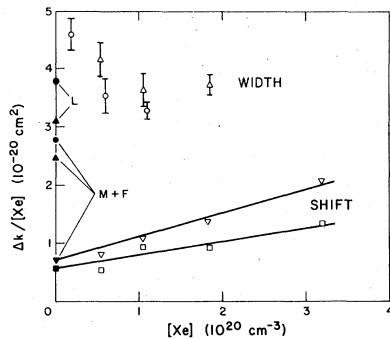


FIG. 5. Broadening rate $\gamma/[Xe]$, where γ is the full width in cm^{-1} for the 590 nm line (Δ) and 596 nm line (\circ). Shift rate $d/[Xe]$ for the 590 nm line (∇) and 596 nm line (\square). The width for $[Xe]=2.2 \times 10^{19} \text{ cm}^{-3}$ is from the wing-intensity analysis in Fig. 4. The values on the $[Xe]=0$ axis are by McCarten and Farr²⁴ (\blacktriangle , \bullet , \blacktriangledown , and \blacksquare for width and shift at 596 nm, and by Lwin *et al.* (\blacktriangle and \bullet for width of 590 and 596 nm). The straight lines fitted to the shift data are for comparison purposes only.

with $[Xe]$. It appears that our data for the shift rate can be fitted, within experimental accuracy, with straight lines whose intercepts are the low-pressure limits measured by McCarten and Farr.

The approximately constant $\gamma/[Xe]$ and linearly varying $d/[Xe]$ might be taken as indicative of predominantly one- and two-Xe interactions, but this may be deceptive. In the impact approximation, collisions with impact parameters greater than the Weisskopf radius R_w are ineffective at broadening, while all closer collisions contribute almost equally; the shift is predominantly due to collisions with impact parameters near R_w .¹ Here $R_w = (\gamma/[Xe]\pi v_0)^{1/2}$, with v_0 the mean interatomic-collision velocity, is the impact parameter that yields unity phase shift and "interruption" of the optical phase. To obtain a constant $\gamma/[Xe]$ and $d/[Xe]$, Na^*-Xe collisions should be independent and not overlap in time. The average number N of perturbers inside R_w at one time is given approximately by $\frac{4}{3}\pi R_w^3 [Xe]$, neglecting effects due to Boltzmann factors associated with the interatomic potentials, and $N \ll 1$ is required for non-overlapping collisions. In the present case $R_w \cong 13 \text{ \AA}$ and $N \cong 2.5$ at our highest $[Xe]=3.2 \times 10^{20} \text{ cm}^{-3}$. The Poisson distribution gives the probability $(N^n/n!) \exp(-N)$ of n -independent perturbers inside R_w , so interactions with more than one or even two Xe at a time inside R_w is highly likely. However, the large frequency shifts associated with these severely broadened lines would appear to be outside the range of validity of the impact approximation, and these large shifts may be primarily due to perturbers at $R < R_w$. Thus the reasons for the observed pressure dependences of $\gamma/[Xe]$ and $d/[Xe]$ are not clear. These highly

qualitative comments, as necessary in the absence of any directly applicable quantitative theory of nonbinary pressure broadening, are intended only to suggest the types of issues involved in interpreting data.

The parameters γ and d completely characterize a Lorentzian broadened line; however, at these high perturber densities the lines are no longer Lorentzian. At the highest density studied, $3.2 \times 10^{20} \text{ cm}^{-3}$, the D lines are broadened to such an extent that their widths are not obtainable. Therefore comparison to theory, when available, should be made using the complete line profile.

B. Secondary satellite

It has been noted that if one assumes additive-pair interactions a satellite feature at $2\Delta k_s$ in the binary (NaXe) spectrum will also appear in the quasistatic spectrum as a weaker satellite at $2\Delta k_s$, due to the triatomic (NaXe_2) spectrum.²⁷ These satellite features will be broadened compared to those given in Fig. 1 of Ref. 27 due to the atomic motion, but the area under each broadened satellite feature must remain nearly the same as that which the quasistatic theory predicts will occur across the same spectral region (e.g. in the present case the region of 590.3–591.7 nm in Fig. 1). The present data at $[Xe]=3.2 \times 10^{20} \text{ cm}^{-3}$ correspond to $V_s[Xe]=0.83$, where $V_s = (4\pi/3)R_s^3$ is the volume inside the satellite radius $R_s = 8.5 \text{ \AA}$, obtained from Ref. 18. The results of Ref. 27 are expressed in terms of $\delta = \frac{1}{32}V_s N$, where N is the perturber density, so to the extent that the 6-12 potential of Ref. 27 is applicable our data correspond to $\delta = 0.026$. From Fig. 1 of Ref. 27 it can be seen that a highly discernable secondary satellite is predicted for δ values in this range. No such feature is apparent in our measured spectrum.

In order to test more quantitatively for a satellite at $2\Delta k_s$ we have carried out an approximate calculation of the spectrum to be expected under the additive-potential assumption. We have utilized Eq. (9) of Ref. 22 to calculate the contribution of the NaXe_2 spectrum to $I_N(k)$ using knowledge of the NaXe spectrum obtained at low $[Xe]$. In essence, the low-pressure limit of $I_N(k)$, which represents the NaXe spectrum, is convoluted with itself. This approximation introduces the motional broadening into the NaXe_2 spectra as convolutions or superpositions of the observed broadening due to single-perturber motion. Royer has derived a similar expression, except utilizing the convolution of quasistatic wings with essentially the broadened line core.²⁸ The predictions of this approximation are compared to the data in Fig. 6. We have included $I_N(k)$ contributions from NaXe and NaXe_2 only, so that the calculated $I_N(\Delta k)$ is

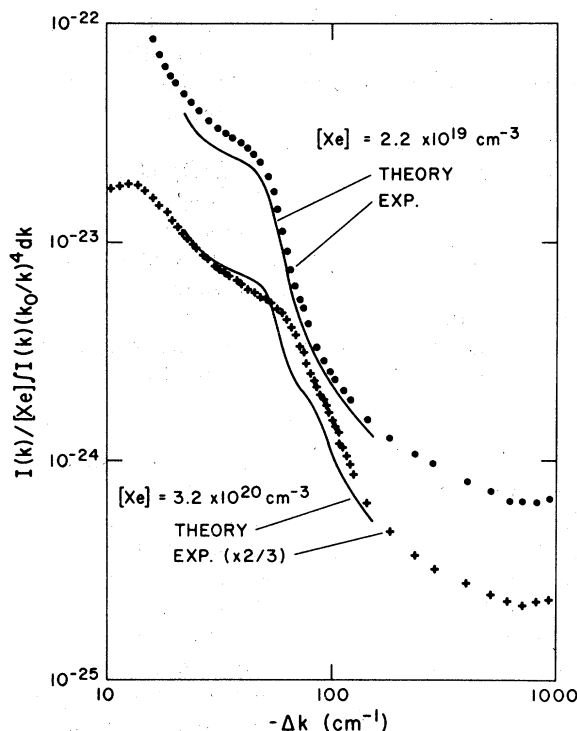


FIG. 6. Normalized Na emission in the presence of $[Xe] = 2.2 \times 10^{19} \text{ cm}^{-3}$ and $3.2 \times 10^{20} \text{ cm}^{-3}$, in the wavelength region of the red satellite. The higher-pressure data have been multiplied by $\frac{2}{3}$ to avoid overlapping the low-pressure data and to facilitate comparison with the theoretical shape. Here Δk is measured from midway between the D lines.

somewhat lower than the measured $I_N(\Delta k)$. The omitted terms, representing NaXe_n ($n > 2$) spectra, are expected to be slowly varying with Δk in the satellite region under investigation, so that they should not affect this comparison of spectral shapes. In this calculation there is some ambiguity in the choice of the unperturbed atomic frequency k_0 , and a value midway between the D lines was chosen. Note the predicted NaXe_2 secondary satellite hump at $\sim -80 \text{ cm}^{-1}$ in the $[Xe] = 3.2 \times 10^{20} \text{ cm}^{-3}$ theoretical spectrum; its intensity is $\sim 10\%$ that of the primary satellite at $\sim -40 \text{ cm}^{-1}$. There is no indication of this secondary satellite in the data.

The relationship between the predicted magnitudes of the primary and secondary satellite is very useful in any search for them. This is easy to see from Eq. (9) of Ref. 22, and is consistent with the results of Ref. 27. In essence, when the area under the primary satellite $I_N(\Delta k_s)W$, where W is the observed satellite width, is a fraction ϵ of the normalized emission, Eq. (9) of Ref. 22 predicts that the area under the secondary satellite will be about $\frac{1}{2}\epsilon^2$. (This is roughly equivalent to the probability of finding two Xe inside R_s , as

given by the Poisson distribution.) Thus, for example, at $[Xe] = 2.2 \times 10^{19} \text{ cm}^{-3}$, a factor of 15 smaller $[Xe]$ than in the above comparison, the secondary satellite is 15 times weaker relative to the NaXe satellite and is no longer visible in the theoretical line in Fig. 6. McCarten and Farr²⁶ have reported a broad hump at $\sim -100 \text{ cm}^{-1}$ in the red wing of the absorption profile of Na perturber by Xe. They have attributed this feature to the (NaXe_2) secondary satellite. However, from the present normalized data it follows that at their perturber density ($3.2 \times 10^{18} \text{ cm}^{-3}$) any such secondary satellite would be about 10^3 lower in intensity than that of the primary satellite; thus it is obviously not the feature reported in Ref. 26. The beginning of the NaXe A-X band absorption, the broadband at -100 to -2000 cm^{-1} in Fig. 2, is probably what was observed.

C. Intensity undulations near satellites

Another aspect of this satellite feature has already been noted in the data section; we do not observe intensity undulations at any pressure, in contradiction to the suggested^{9,10} shapes for broadening of Cs resonance lines by high-pressure Xe. This supports the suggestion in Ref. 3 that realistic potentials and considerable computational care are necessary for such calculations.

D. Conclusions

The qualitative behavior of the far-wing intensities as a function of perturber density can be understood in terms of the depletion of free Na^* due to molecular formation and the more spread out character of the NaXe_n spectra as n increases. These effects are predicted by the additive-interaction model as given in Eq. (9) of Ref. 22. However, the behavior is not well understood quantitatively. In particular, we do not observe a secondary satellite or intensity undulations in the neighborhood of the red satellite, nor has the pressure dependence of $I_N(k)$ been calculated. The line-core shifts and widths appear to have a very simple $[Xe]$ dependence, for unknown reasons.

ACKNOWLEDGMENTS

We wish to thank Richard Scheps for major contributions during the construction stages of the experiment, and Jinx Cooper for valuable comments. This work was supported by the Air Force Weapons Laboratory under Grant No. AFWL 77-010, and the Advanced Research Projects Agency of the Department of Defense monitored by the Office of Naval Research under Contract No. N00014-76-C-0123.

- *Present address: Physics Dept., Univ. of California, Santa Barbara, Calif. 93106.
- †Staff member, Quantum Physics Division, National Bureau of Standards.
- ¹S. Y. Chen and M. Takeo, *Rev. Mod. Phys.* **29**, 20 (1957).
- ²J. Szudy and W. E. Baylis, *J. Quant. Spectrosc. Radiat. Transfer* **15**, 641 (1975).
- ³J. F. Kielkopf, *J. Phys.* B **9**, 1601 (1976).
- ⁴J. R. Fuhr, W. L. Wiese, and L. J. Roszman, *Bibliography on Atomic Line Shapes and Shifts*, Natl. Bur. Stand. Spec. Publ. No. 366 (U.S. GPO, Washington, D.C., 1972); *ibid.*, Suppl. 1 (1974); *ibid.*, Suppl. 2 (1975).
- ⁵E. A. Andreev, *Opt. Spektrosk.* **34**, 603 (1973) [*Opt. Spectrosc.* **34**, 346 (1973)].
- ⁶L. M. Sando and J. C. Wormhoudt, *Phys. Rev. A* **7**, 1889 (1974); K. Sando, *ibid.* **9**, 1103 (1974).
- ⁷J. Cooper, "Comments on the Theory of Satellite Bands," Report No. 111 (1973), Joint Institute for Laboratory Astrophysics, University of Colorado, Boulder, Colorado 80309 (unpublished).
- ⁸P. W. Anderson, *Phys. Rev.* **86**, 809 (1952); **76**, 647 (1949); P. W. Anderson and J. D. Talman, *Bell Tel. Syst. Tech. Publ. No. 3117* (unpublished).
- ⁹M. Takeo, *Phys. Rev. A* **1**, 143 (1970).
- ¹⁰N. F. Allard and S. Sahel-Brechot, *Phys. Lett.* **48A**, 135 (1974); N. F. Allard, S. Sahel-Brechot, and Y. G. Biraud, *J. Phys.* B **7**, 2158 (1974).
- ¹¹J. Kieffer, *J. Chem. Phys.* **51**, 1852 (1969).
- ¹²A. Royer, *Phys. Rev. A* **3**, 2044 (1971).
- ¹³A. Jablonski, *Acta Phys. Pol.* **23**, 493 (1963).
- ¹⁴E. Czuchaj, *Acta Phys. Pol. A* **5**, 97 (1974), and references therein.
- ¹⁵R. W. Davies, *Phys. Rev. A* **12**, 927 (1975).
- ¹⁶H. Jacobson, *Phys. Rev. A* **5**, 989 (1972).
- ¹⁷W. E. Baylis, *J. Chem. Phys.* **51**, 2665 (1969).
- ¹⁸J. Pascale and J. Vandeplanque, *J. Chem. Phys.* **60**, 2278 (1974).
- ¹⁹N. Lwin, D. G. McCarten, and E. L. Lewis, *J. Phys.* B **9**, L161 (1976).
- ²⁰R. B. Bernstein and J. T. Muckerman, in *Advances in Chemical Physics*, edited by J. O. Hirschfelder (Wiley, New York, 1967), Vol. 12.
- ²¹G. York, R. Scheps, and A. Gallagher, *J. Chem. Phys.* **63**, 1052 (1975).
- ²²W. P. West, P. Shuker, and A. Gallagher, *J. Chem. Phys.* (to be published).
- ²³J. Carlsten and A. Szoke, *Phys. Rev. Lett.* **36**, 667 (1978).
- ²⁴C. G. Carrington and A. Gallagher, *Phys. Rev. A* **10**, 1464 (1974).
- ²⁵G. Moe, A. C. Tam, and W. Happer, *Phys. Rev. A* **14**, 349 (1976).
- ²⁶D. G. McCarten and J. M. Farr, *J. Phys.* B **9**, 985 (1976).
- ²⁷W. R. Hindmarsh and J. M. Farr, *J. Phys.* B **2**, 1388 (1969).
- ²⁸A. Royer, *Phys. Rev. A* **3**, 2044 (1971).